JOURNAL OF MATERIALS SCIENCE 29 (1994) 921–928

Toughness characterization of niobium-bearing HSLA steels

K. K. Ray, D. Chakraborty
Department of Metallurgical Engineering, Indian Institute of Technology, Kharagpur, India 721302

S. Ray
Scientific Services Division, The Tata Iron and Steel Co. Ltd, Jamshedpur, India 831007

Estimates of toughness in terms of Charpy impact energy and the critical stress intensity factor, K_{ICV} using deeply chevron-notched specimens were made for two casts of niobium-bearing high-strength low-alloy (HSLA) steels. K_{ICV} determinations are carried out for the first time using both three- and four-point bend loading configurations for this material. Quantitative analyses of the material microstructures are made with respect to the amount of the phases, ferrite grain size, and the volume fraction, length, aspect ratio, and mean inter-spacings of the inclusions. A comparative study of impact and fracture toughness with regard to the microstructural parameters, indicates that the latter toughness characterization approach is far superior to the former. The compatibility of the estimated values of K_{ICV} using the two different loading configurations is discussed.

1. Introduction

There has been a steady growth in the production of microalloyed steels over the last two decades, currently reaching a figure of approximately 10% of the total world market for constructional steels [1]. The steady development of this material and the keen interest in its structure–property relations with attendant variations in its chemistry, production steps and forming practices are well cited with the several international conferences [2–6] held over recent years. A severe demand for an understanding of fracture toughness of this material in relation to its microstructural aspects exists in the industries, in order to implement quality control of toughness using fracture mechanics principle. But very little information on K_C [7], K_{IC} [8], $K_{IC}(J)$ [9] or COD [10] is available for this type of material. The present investigation aimed to deal with some of these aspects.

The common varieties of high-strength low-alloy (HSLA) steel plates are generally produced in the thickness range 6–80 mm, and these are associated with strength and toughness properties in such a way that estimation of K_{IC} using linear elastic fracture mechanics (LEFM) is often not possible. The use of elastic plastic fracture mechanics (EPFM) criteria for industrial quality control of toughness also do not appear to bear enough potential. As a consequence, impact toughness characterization using Charpy V-notched specimens is currently the most popular approach for quality control of the toughness of HSLA steels. On the other hand, fracture toughness evaluation using chevron-notched specimens [11, 12] is an emerging technique which possesses several advantages over the conventional methods, and primarily for its simplicity attempts are being made to develop it for quality control of commercial structural materials. Recently, some of the present authors have emphasized probing the potential of using K_{ICV} for quality control of HSLA steels [13].

The suggested principles of Barker [11] and several other early workers [14–17] point out that the unique feature of chevron-notched specimens is the presence of an extremely high stress concentration at the notch tip, which guides the crack path. Four variations in this test technique have emerged, which can be categorized as: (a) short rod [18–28], (b) short bar [26–34], (c) three-point bend (TPB) [35–41], and (d) four-point bend (FPB) [41–45] tests. A schematic configuration of a bend bar specimen is shown in Fig. 1 and the expression used for estimating fracture toughness using such a specimen is as follows

$$K_{ICV} = \frac{P_{max} Y^*_{min}}{B W^{1/2}} \quad (1)$$

where B and W are defined in Fig. 1, P_{max} is the maximum load encountered during such a test, and Y^*_{min} is the normalized stress intensity factor.

The computation of the normalized stress intensity factor can be carried out in different ways [12], but for bend bars this can be easily estimated using the suggested approaches of Wu Shang-Xian [40] or Withey and Bowen [45]. Using bend bar specimen configuration having $B:W:S$ ratio of 1:1.5:6, attempts have been made to estimate K_{ICV} together with theoretical estimation of Y^*_{min} following existing approaches [40, 45]. The major aims of this investigation were: (i) to make an assessment of K_{ICV} of niobium-bearing

0022–2461

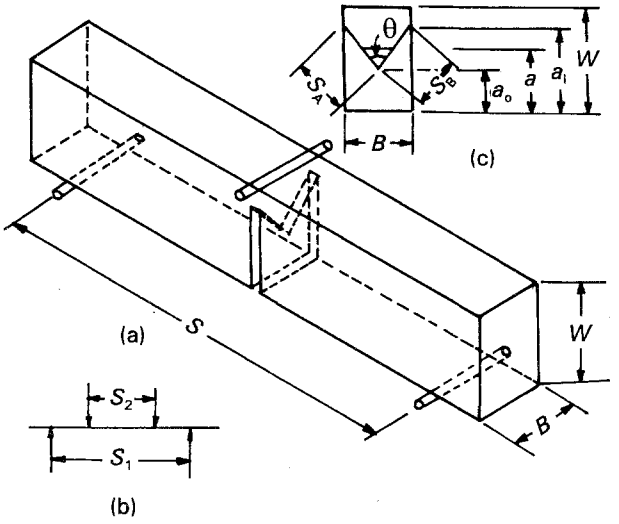

Figure 1 Geometry of chevron-notched bend specimen under (a) three-point loading configuration, (b) four-point loading configuration, and (c) notch plane section. B = specimen thickness, W = specimen width, S = span for three-point loading, S_1 and S_2 = shorter and longer spans for four-point loading, a_0 = initial crack length, a = crack length, a_1 = surface chevron notch length, θ = slot angle, S_A and S_B = side lengths of the chevron notch).

HSLA steels using TPB and FPB loading configurations in order to examine the compatibility of these test techniques, and (ii) to understand impact and fracture toughness properties with regard to the microstructure and the cleanliness indices of the materials.

2. Experimental procedure

The primary emphasis in this investigation was to estimate K_{ICV}, for which no International Standard exists. An estimate of the specimen thickness B for K_{IC} test following the equation [8]

$$B \geq 2.5(K_Q/\sigma_y)^2 \quad (2)$$

yields $B > 120$ mm for the expected level of yield strength, $\sigma_y = 460$ MPa and the apparent fracture toughness, $K_Q \simeq 100$ MPa m$^{1/2}$, of the investigated material. But the commercial steel plates were 16 mm thick, indicating the impossibility of K_{IC} estimation. The thickness criterion of K_{IC} specimens is primarily based on the concept of plastic zone associated with the crack tip [46]. The principle of K_{ICV} estimation [11] is distinctly different than that of K_{IC} determination, and hence any similar assessment of specimen thickness for this test is not possible. Only for short-rod specimens, has Barker [24] suggested some empirical formulation based on experimental results, to decide the specimen diameter, which is again not applicable for bend bar specimens. To arrive at a specimen thickness which can give a K_{ICV} value comparable to an appropriate K_{IC} value, it was thus decided to follow the specimen geometry suggested by Wu Shang-Xian [35] for bearing steels.

2.1. Steels tested

The compositions of the steels with their code numbers are shown in Table I, for which the equivalent Indian, British and American standard specifications are IS 8500-1977, BS 4360-1990 and A 572-88, respectively. The as-received commercial steel plates were from semi-killed ingots and were in the air-cooled condition from the finishing rolling temperature of ≈ 1223 K.

TABLE I Composition of the steels

Material code	Elements (wt %)					
	C	Mn	S	P	Si	Nb
Cast A	0.19	1.59	0.028	0.034	0.042	0.024
Cast B	0.19	1.58	0.028	0.028	0.050	0.032

2.2. Microstructural examination

Representative specimens from each cast were prepared for metallographic examination using 2% initial etchant. The volume fractions, V_f, of the phases (ferrite and pearlite) were determined using the point-counting technique [47]. A 10×10 grid was used at a magnification of $\times 400$, and random countings on 25 fields of observation were made.

The ferrite grain sizes of the materials were obtained with the help of linear intercept method for two-phase structures [47], by viewing the microstructure at a magnification of $\times 400$. A total number of 50 random intercepts were considered for obtaining the average number of ferrite grains per test line. Using the volume fraction of ferrite, V_α and the average number of ferrite grains, N_α, intercepted by the test line, the mean grain size, L, was calculated with the help of the equation [47]

$$L = (V_\alpha L_T / N_\alpha) \quad (3)$$

where L_T is the length of the superimposed grid line.

2.3. Inclusion characterization

Quantitative ratings of inclusions included the following assessments: (a) determination of volume fraction, (b) obtaining the average size and aspect ratio of the sulphide inclusions, and (c) estimating the nearest neighbour inter-inclusion spacings. Samples, collected from four locations, were soaked at 1123 K for 20 min and were water-quenched before preparing the highly polished metallographic specimens for inclusion ratings in the unetched condition. The average inclusion rating assessments were made for both longitudinal and transverse directions of the steel plates.

The volume fraction of inclusions was determined using the Japanese standard method JIS 0555 [48]. The average length and aspect ratio of the inclusions were estimated from the measurement of length and width of the elongated sulphide inclusions using the cursors of a LECO microhardness tester. For each sample, 100 randomly selected inclusions were characterized, and the data were computed to obtain the average size, size distribution and the aspect ratio of the inclusions. The estimation of the inter-inclusion spacings was also carried out using the measurement

facilities of the same microhardness tester. In this measurement, with reference to a marked inclusion, all the nearest neighbour inclusion distances were measured, out of which the smallest reading was considered as the inter-inclusion spacing. The separation between two inclusions is defined as the centre-to-centre radial distance in this assessment. In each sample, 50 such readings were taken to compute the mean inter-inclusion spacing; a separate record of the smallest reading out of these measurements was also made.

2.4. K_{ICV} test

Deeply chevron-notched bend (DCNB) type specimens, as shown in Fig. 1, were used for fracture toughness testing. The dimensions of the TPB specimens were $B = 12$ mm, $W = 18$ mm, and $S = 72$ mm. For FPB specimens the longer and the shorter span lengths were 72 and 36 mm, respectively. However, the total length of the specimens was kept as 130 mm with the specific objective that Charpy specimens can be made from the broken halves of the K_{ICV} specimens, after cutting the fracture surfaces for SEM examination. The slit width of chevron notches was cut in two steps, initially with 1 mm thickness followed by the final 1 mm depth using 0.3 mm thickness. All K_{ICV} specimens conformed to the T–L orientation. For K_{ICV} estimation, the specimens were loaded either in a three-point or in a four-point bend fixture of an Instron machine (1344 series). The specimens were loaded at a crosshead velocity of 1 mm min^{-1} at the room temperature of 295 K, and the load–displacement diagrams were recorded to estimate the maximum load during such a test for evaluating K_{ICV} using Equation 1.

2.5. Tensile and Charpy test

Flat tensile specimens with a gauge length of 200 mm and width 40 mm were cut from as-received plate in the transverse direction as per ASTM standard E8-87 [49]. The tensile tests were performed at a nominal strain rate of $\approx 3 \times 10^{-3}\,s^{-1}$, in a universal testing machine. The 0.2% offset yield strength, the ultimate tensile strength and the percentage elongations were obtained from the test results at the room temperature of 300 K.

Impact tests were carried out on standard Charpy V-notch bars of 55 mm length as per ASTM specification E23-86 [50], in the T–L orientation. These tests were carried out at a room temperature of 300 K using a pendulum impact testing machine (PSW 30, Mohr and Federuaff AG, Mannham, Germany).

2.6. Fractographic examination

The fractured surfaces of several K_{ICV} specimens were examined using an SEM (model CamScan series 2DV). The entire fracture surface of each specimen was scanned at different magnifications and a series of representative fractographs were taken.

3. Results

3.1 Metallographic examination

The metallographic examination of etched samples revealed that the ferrite grains are virtually equiaxed as shown in Fig. 2. The volume fraction of pearlite and the average ferrite grain size in the two casts are similar as seen from Table II. Theoretical estimate of the volume fraction of pearlite from the iron–carbon phase diagram for 0.19% C steel is 21.8%. The observed higher volume fraction of pearlite results due to the presence of the alloying elements and the non-equilibrium normalized states of the microstructures. The average grain size of the two casts as reported in Table II, correspond to ASTM grain sizes between 11 and 12, which are common for HSLA steels.

A typical representative photograph showing inclusions in longitudinal section is shown in Fig. 3. The inclusion morphology in the transverse direction was

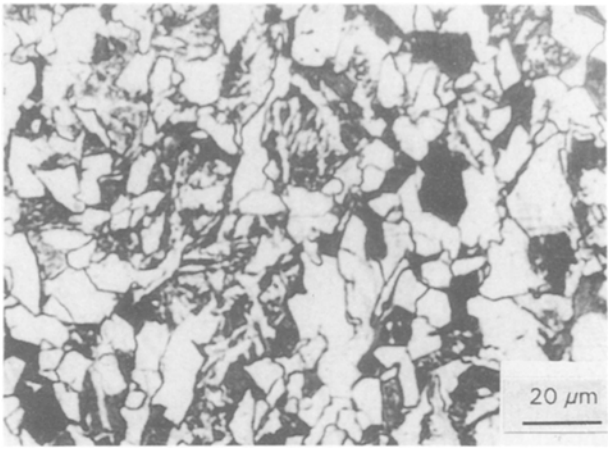

Figure 2 A typical representative microstructure of the investigated materials showing primarily a mixture of equiaxed ferrite and pearlite along with some accicular ferrite.

TABLE II Microstructural aspects

Material code	Volume fraction of pearlite (%)	Grain size of ferrite (μm)
Cast A	29.3	7.14
Cast B	29.6	7.07

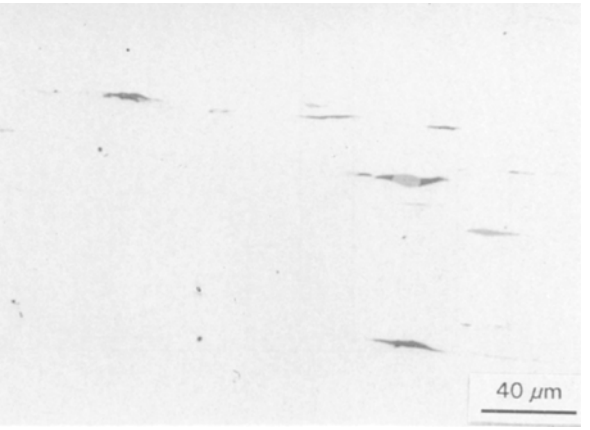

Figure 3 A typical photograph showing elongated sulphide inclusions in the longitudinal direction.

TABLE III Inclusion characterization

Parameters		Cast A		Cast B	
		L	T	L	T
Inclusion vol. fraction (%)	1.	0.7 ± 0.15	0.4 ± 0.10	0.7 ± 0.12	0.2 ± 0.05
	2.	0.2 ± 0.05	0.3 ± 0.07	0.3 ± 0.07	0.2 ± 0.06
Mean length of inclusions (μm)	1.	17.4 ± 1.7	9.9 ± 1.10	20.1 ± 1.9	11.7 ± 0.9
	2.	20.8 ± 2.8	9.7 ± 0.8	21.3 ± 1.9	12.0 ± 1.3
Max. length of inclusions (μm)	1.	44.5	40.9	70.1	28.8
	2.	82.4	24.3	52.9	42.0
Mean aspect ratio	1.	3.4 ± 0.33	2.3 ± 0.19	5.0 ± 0.43	4.0 ± 0.36
	2.	8.4 ± 2.10	2.5 ± 0.17	5.5 ± 0.76	3.1 ± 0.21
Mean inter-inclusion spacing (μm)	1.	52.8 ± 10.4	36.6 ± 8.8	30.4 ± 4.9	20.3 ± 4.2
	2.	32.5 ± 7.6	13.5 ± 2.3	26.5 ± 4.4	9.6 ± 1.8
Min. inter-inclusion spacing (μm)	1.	6.7	6.0	4.0	1.7
	2.	2.6	1.2	6.2	1.1

also of similar nature with a difference in aspect ratio because of the cross-rolled condition of the material. The estimated average magnitudes of volume fraction, size, aspect ratio and inter-spacings of inclusions on two specimens in both longitudinal and transverse directions per cast are given in Table III together with their errors of 95% confidence level. In addition, a typical histogram of inclusion length distribution is presented in Fig. 4.

3.2. Mechanical properties

Tensile and Charpy tests were conducted on three samples taken from each cast. Average tensile and impact properties for these materials are reported in Table IV. The tensile properties are in good agreement with the ones reported in the literature [13, 51] for similar chemistry of materials.

TABLE IV Tensile and impact properties

Material code	Tensile properties		Charpy impact energy
Cast A	Yield strength	= 460 MPa	29.8 ± 3.0 J (30.4, 26.5, 32.4 J)
	Ultimate tensile strength	= 598 MPa	
	% elongation	= 20.7	
Cast B	Yield strength	= 463 MPa	44.8 ± 7.5 J (38.3, 43.2, 53.0 J)
	Ultimate tensile strength	= 615 MPa	
	% elongation	= 20.0	

3.3. Fracture toughness

A total of eight fracture toughness specimens pertaining to casts A and B were tested under both TPB and FPB loading configurations; one sample being tested at a high crosshead velocity of 180 mm min^{-1}. The photographs of a set of fractured surfaces are shown in Fig. 5. The dimensions a_0, S_1 and S_2 (Fig. 1) were measured from the broken halves of the fractured samples, using which Y^*_{min} values were calculated. Any asymmetric notch showing more than 3% deviation between S_1 and S_2 was excluded from the present report. The detailed dimensions of the specimens along with the normalized stress intensity factors are given in Table V, whereas the recorded load and the estimated K_{ICV} values are given in Table VI. The

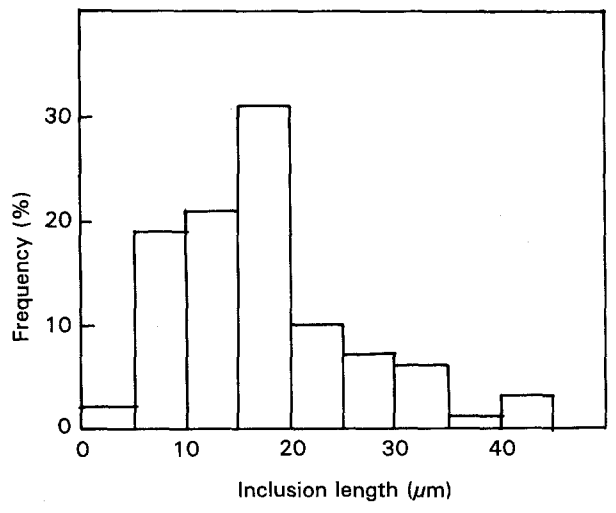

Figure 4 A representative histogram of the lengths of sulphide inclusions in the investigated materials.

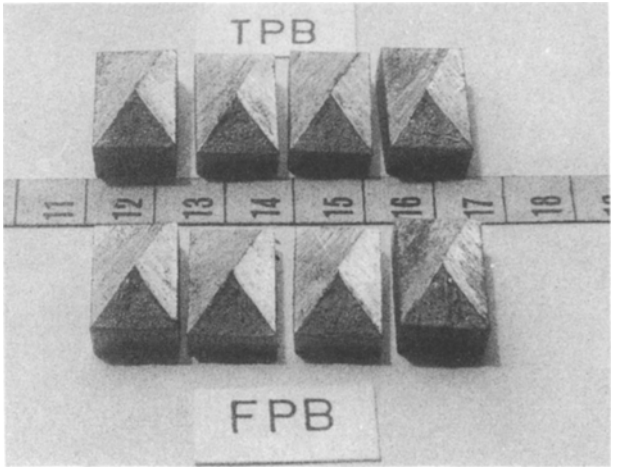

Figure 5 Typical broken surfaces of fracture toughness test specimens under three-point bend (TPB) and four-point bend (FPB) loading modes.

TABLE V Characteristic dimensions of the specimens and Y^*_{min} values

Strain rate (mm min^{-1})	Specimen	Span length (mm)	B (mm)	W (mm)	a_0 (mm)	S_1 (mm)	S_2 (mm)	Type of test	Y^*_{min} from	
									a_0	S_1 and S_2
1	A1	72	11.98	18.0	7.39	11.96	11.96	TPB	26.25	28.29
	B1	72	11.89	18.0	7.26	12.39	12.48	TPB	26.75	26.06
	A2	72	11.95	18.0	7.03	12.33	12.06	FPB	13.37	13.19
	B2	72	11.99	17.99	7.44	12.33	12.37	FPB	14.10	13.67
	B3	72	11.90	17.91	7.26	12.17	12.14	FPB	13.90	14.01
180	A5	72	11.92	17.98	7.96	11.96	11.99	FPB	15.20	14.43

TABLE VI Calculated fracture toughness values of specimens

Strain rate (mm min^{-1})	Type of test	Specimen	P_{max} (kg)	K_{ICV} (MPa m$^{1/2}$) from		
				a_0	S_1 and S_2	Average
1	TPB	A1	560	93.1	96.7	94.9
	TPB	B1	565	92.9	90.5	91.7
	FPB	A2	1110	90.9	89.6	90.3
	FPB	B2	1110	95.5	92.5	94.0
	FPB	B3	1150	98.5	99.2	98.9
180	FPB	A5	1140	106.3	100.9	103.6

maximum error associated with K_{ICV} estimation is $\leq 4.0\%$. For a comparative study of the fracture and impact toughness, a histogram of all estimated K_{ICV} and Charpy energy values are made in Fig. 6.

3.4. Fractography

The crack path of broken chevron-notched specimens revealed quasi-cleavage fracture with tear ridges similar to those observed by Lazaridis and Margonon [52] as shown in Fig. 7. At localized regions, distinct transgranular cleavage showing river lines were also observed as shown in Fig. 8. Interestingly it was observed that cavities are formed around elongated sulphide inclusions, but instead of having any microvoid coalescence, these are associated with either cleavage planes or tear ridges in their neighbourhood.

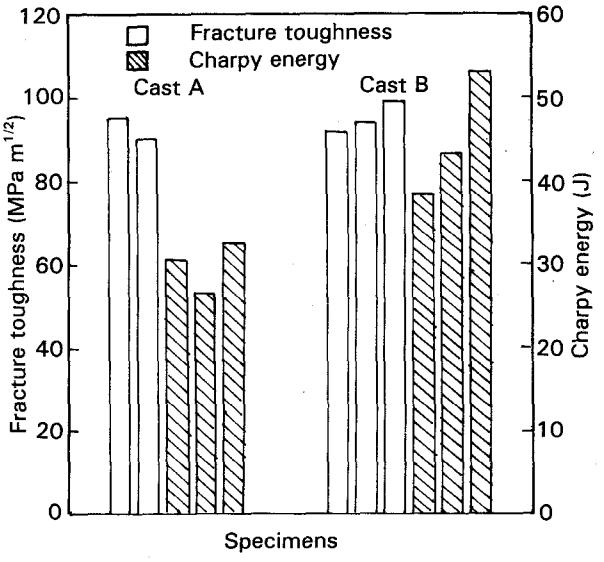

Figure 6 Histogram of fracture toughness, K_{ICV}, and Charpy energy values of the tested specimens.

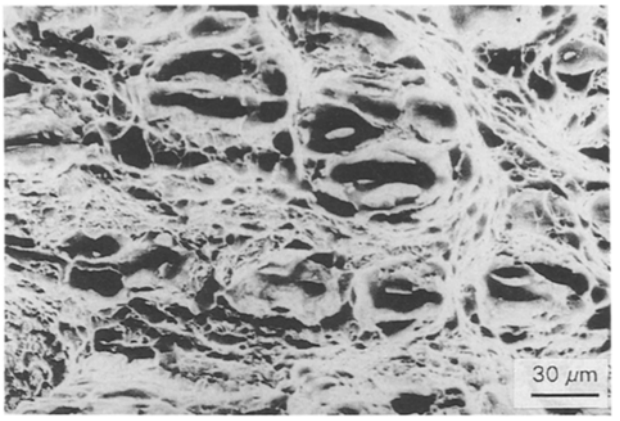

Figure 7 A typical region of quasi-cleavage fracture showing embedded inclusions and tear ridges.

Figure 8 An enlarged view of a localized transgranular fracture showing river lines.

4. Discussion

The contents of this section emphasize the elucidation of two distinct aspects: (a) the usefulness and reliability of K_{ICV} determined by different loading configurations, and (b) the influence of material characteristics

on toughness determined by impact and fracture mechanics approaches.

4.1. Estimation of K_{ICV} using TPB and FPB loading

The calculation of K_{ICV} is based on Equation 1 in which P_{max}, B and W are experimental parameters, whereas Y^*_{min} is a theoretical estimate based on specimen-crack configuration. The computations of Y^*_{min} have been carried out following the work of Wu Shang-Xian [40] and Withey and Bowen [45]. The developed softwares for these computations were first examined to check some reported results by the earlier investigators [40, 45]. It was noted that the Y^*_{min} computed by the developed softwares deviates from the results of Wu Shang-Xian [40] by less than 0.2% and from the results of Withey and Bowen [45] by less than 0.6%. Such deviations are attributed to the truncation error in such computations and hence the developed softwares for Y^*_{min} calculations are in excellent agreement with the earlier reports.

Estimation of Y^*_{min} requires the notch parameter a_0, as shown in Fig. 1. It was experienced while performing these tests that a_0 can be either estimated directly or can be calculated from the length of the sides of the triangular fracture surfaces. The magnitudes of Y^*_{min} for all samples were computed using both sets of measurements. Table V indicates that computed Y^*_{min} values from the two modes of calculations are in good agreement, except in one specimen. This exception is attributed to the uncertainty in locating the exact notch tip, which occurs at times. Thus estimation of Y^*_{min} from this two-fold approach becomes a self-checked parameter. An average of the estimated K_{ICV}, based on the two approaches of Y^*_{min} calculations, is considered to represent the fracture toughness of a specimen.

Table VI gives the average fracture toughness values of the two casts A and B as 92.6 and 94.9 MPa $m^{1/2}$, respectively. It is interesting to note that using the same loading rate, specimens A2, B2 and B3 were tested under FPB loading unlike TPB loading for A1 and B1; but the deviation due to change in mode of loading is not distinguishable within the possible scatter band of these results. This leads us to conclude that estimation of fracture toughness from chevron-notched bend bar specimens is not dependent on the loading configurations. Fractographic examinations of broken TPB and FPB specimens also did not reveal any distinctive feature for these two loading configurations.

Testing of specimen A3 at high strain rate was made to check the possible effect of strain rate on this type of testing. This test indicates that K_{ICV} is increased by approximately 11 MPa $m^{1/2}$ when the strain rate is changed by 180 times. The effect of strain rate on K_{ICV} estimation using chevron-notched specimens has not been reported so far in the literature, but the variation of fracture toughness with loading rate for conventional testing [53] indicates that this property first decreases and then increases with increasing loading rate. So no definite conclusion could be drawn from the limited result, and this aspect is currently being investigated.

Fracture toughness data using conventional tests [7–10] are not available for this material. Using Sailors and Corten's [54] empirical relationship between Charpy energy and fracture toughness, it was estimated that the magnitude of K_{IC} for casts A and B should be in the range 75.2–83.1 and 90.3–106.3 MPa $m^{1/2}$, respectively. This order of fracture toughness values, though not accurate, supports the magnitude of the evaluated K_{ICV} values. In addition, Klassen *et al.* [55] have suggested that the J_{IC} of HSLA steels can be empirically correlated with the grain size, inclusion diameter and the percentage inclusion volume fraction. Following Fig. 15 of [55] and considering maximum inclusion length instead of inclusion diameter, the magnitude of J_{IC} for casts A or B should be 50.8 and 54.0 kJ m^{-2}, which corresponds to K_{IC} values of 103.3 and 106.5 MPa $m^{1/2}$. These estimates are also in good agreement with the obtained magnitudes of the K_{ICV} for the investigated steels.

4.2. Impact and fracture toughness versus material characteristics

The average fracture toughness value of cast A (92.6 MPa $m^{1/2}$) is marginally lower than that of cast B (94.9 MPa $m^{1/2}$) whereas the average Charpy impact energy of cast A (29.8 J) is significantly different from that of cast B (44.8 J). In addition, Fig. 6 indicates that the Charpy energy values are associated with a larger scatter band compared to those of K_{ICV} values. The variations in the chemistry (Table I) and microstructural aspects (Table II) of the two casts are too negligible to reflect any change in their toughness characteristics. However, apparently there exists some differences in the inclusion characterizing parameters of the two casts, as given in Table III.

Cast A, having higher inclusion volume percentage, higher maximum inclusion length and smaller inter-inclusion spacings, is expected to have lower toughness [55–57] as indicated by Charpy energy results. But the differences in the inclusion characterizing parameters of the two materials are often in the scatter band of measurement. Hence, it is difficult to support the larger observed difference in Charpy impact energy. On the other hand, following Klassen *et al.* [55] the difference between the fracture toughness values of the two casts should not exceed 3.2 MPa $m^{1/2}$ based on the inclusion characterizing parameters. This is in agreement with the difference in the average K_{ICV} values of the two casts. The present results thus clearly indicate that impact toughness characterization, though popular in industrial practice, could be highly dangerous for ascertaining resistance to fracture of a material.

5. Conclusions

The following major conclusions can be drawn from the results of this investigation.

1. Fracture toughness values of HSLA steels have been estimated for the first time using chevron-notched bend bars under both three- and four-point loading configurations. The estimated values of K_{ICV} from the different loading configurations are in excellent agreement and their order is also in good agreement with indirect assessments.

2. The fracture toughness values of two casts of HSLA steels are found to be 92.6 and 94.6 MPa $m^{1/2}$, compared with their corresponding average Charpy energy values of 29.8 and 44.8 J, respectively. The overall variations in chemistry, microstructural aspects and inclusion characterizing parameters of the two casts can explain the difference in K_{ICV} values, but are unable to justify the large variation in the Charpy energy values. This fact warns that toughness characterization for varying material characteristics using Charpy impact test could result in misleading inferences.

Acknowledgements

The authors thank The Tata Iron and Steel Co. Ltd, Jamshedpur, India, for supplying the research materials and for sponsoring one of the authors for this research programme. The authors also thank Mr S. Dutta and Mr A. S. Banerjee for their assistance in the experimental work.

References

1. J. H. WOODHEAD and S. R. KEOWN, in "HSLA Steels-Metallurgy and Applications", edited by J. M. Gray, T. Ko, Zhang Shouhua, Wu Baorong, Xie Xishan (ASM International, 1986) p. 15.
2. J. CRANE (ed.), Proceedings of an International Symposium on HSLA steels, Microalloying 75, Washington DC, October 1–3, 1975 (John Crane, Union Carbide Corporation, Metals Division, Washington, DC 1977).
3. M. KORCHYNSKI (ed.), "Proceedings of an International Conference on HSLA Steels Technology and Applications", Philadelphia, PA, October 1983, (Union Carbide Corporation, 1984).
4. J. M. GRAY, T. KO, ZHANG SHOUHUA, WU BAORONG, XIE XISHAN (eds), "Proceedings of an International Conference on HSLA Steels' 85", Beijing, China, November 4–8, 1985 (ASM International, Beijing, 1986).
5. A. T. DAVENPORT (ed.), Proceedings of a Symposium on Formable HSLA and Dual Phase Steels, Chicago, IL, October 26, 1977, (Metallurgical Society of AIME, Chicago, IL, 1979).
6. "Proceedings of an International Conference on HSLA Steels' 90", Beijing, China, October 28–November 2, 1990 (TMS, USA).
7. American Society for Testing of Materials, "Standard Practice for R-Curve determination," E561-86 (ASTM, Philadelphia, PA, 1986).
8. American Society for Testing of Materials, "Plane Strain Fracture Toughness for Metallic Materials," E399-83 (ASTM, Philadelphia, PA, 1983).
9. American Society for Testing of Materials, "Standard Test Method for J_{IC} A Measure of Fracture Toughness", E813-87 (ASTM, Philadelphia, PA, 1987).
10. British Standards Institution, "Methods for Crack Opening Displacement (COD) Testing", BS 5762 (1979).
11. L. M. BARKER, *Eng. Fract. Mech.* **9** (1977) 361.
12. J. C. NEWMAN Jr, in "Chevron Notched Specimens: Testing and Stress Analysis," ASTM STP 855, edited by J. H. Underwood, S. W. Freiman and F. I. Baratta (American Society for Testing and Materials, Philadelphia, PA, 1984) p. 5.
13. K. K. RAY and S. RAY, in "Proceedings of International Symposium on Fatigue and Fracture in Steel and Concrete Structures", Madras, December 1991, edited by A. G. Madhava Rao and T. V. S. R. Appa Rao (Oxford and IBH, New Delhi, 1991) p. 317.
14. J. NAKAYAMA, *Jpn J. App. Phys.* **3** (1964) 422.
15. H. G. TATTERSALL and G. TAPPIN, *J. Mater. Sci.* **1** (1966) 296.
16. L. P. POOK, *Int. J. Fract. Mech.* **8** (1972) 103.
17. J. I. BLUHM, *Eng. Fract. Mech.* **7** (1975) 593.
18. L. M. BARKER and F. I. BARATTA, *J. Test. Eval.* **8** (1980) 97.
19. J. L. SHANNON Jr, R. T. BUBSEY, W. S. PIERCE and D. MUNZ, *Int. J. Fract.* **19** (1982) R55.
20. J. F. BEECH and A. R. INGRAFFEA, *ibid* **18** (1982) 217.
21. L. M. BARKER, in "Fracture Mechanics of Ceramics", Vol. 3, edited by R. C. Bradt, D. P. H. Hasselman and F. F. Lange (Plenum Press, New York, 1978) p. 483.
22. L. M. BARKER and W. C. LESLIE, in "Advances in Research on the Strength and Fracture of Materials", Vol. 2A, edited by D. M. R. Taplin (Pergamon Press, New York, 1977) p. 98.
23. D. MUNZ, *Eng. Fract. Mech.* **15** (1981) 231.
24. L. M. BARKER, in "Chevron Notched Specimens: Testing and Stress Analysis", ASTM STP 855, edited by J. H. Underwood, H. W. Freiman and F. I. Baratta (American Society for Testing and Materials, Philadelphia, PA, 1984) p. 117.
25. J. HONG and P. SCHWARZKOPF, *ibid.*, p. 297.
26. WANG CHIZHI, YUAN MAOCHAN and CHEN TZEGUANG, *ibid*, p. 193.
27. K. R. BROWN, *ibid.*, p. 237.
28. J. L. SHANNON and D. G. MUNZ, *ibid*, p. 270.
29. J. ESCHWEILER, G. MARCI and D. G. MUNZ, *ibid.*, p. 255.
30. A. MENDELSON and L. J. GHOSN, *ibid.*, p. 69.
31. R. J. SANFORD and R. CHONA, *ibid.*, p. 81.
32. L. M. BARKER, in "Short Rod and Short Bar Fracture Toughness Specimen Geometries and Test Methods for Metallic Materials", ASTM STP 743, edited by R. Roberts (American Society for Testing and Materials, Philadelphia, PA, 1981) p. 456.
33. *Idem*, in "Fracture Mechanics Applied to Brittle Materials", ASTM STP 678, edited by S. W. Freiman (American Society of Testing and Materials, Philadelphia, PA, 1979) p. 73.
34. D. MUNZ, R. T. BUBSEY and J. L. SHANNON Jr, *J. Test. Eval.* **8** (1980) 103.
35. WU SHANG-XIAN, *Eng. Fract. Mech.* **19** (1984) 221.
36. T. T. SHIH, *ibid.* **14** (1981) 821.
37. *Idem, J. Test. Eval.* **9** (1981) 50.
38. WU SHANG-XIAN, *Int. J. Fract.* **19** (1982) R27.
39. L. CHUCK, E. R. FULLER Jr and S. W. FREIMAN, in "Chevron Notched Specimens: Testing and Stress Analysis", ASTM STP 855, edited by J. H. Underwood, S. W. Freiman and F. I. Baratta (American Society for Testing and Materials, Philadelphia, PA, 1984) p. 167.
40. WU SHANG-XIAN, *ibid.*, p. 176.
41. I. BAR-ON, F. R. TULER and I. ROMAN, *ibid.*, p. 98.
42. R. F. KRAUSE Jr and E. R. FULLER Jr, *ibid.*, p. 309.
43. D. MUNZ, R. T. BUBSEY and J. L. SHANNON Jr, *J. Am. Ceram. Soc.* **63** (1980) 300.
44. D. G. MUNZ, J. L. SHANNON Jr and R. T. BUBSEY, *Int. J. Fract.* **16** (1980) R137.
45. P. A. WITHEY and P. BOWEN, *ibid.* **46** (1990) R55.
46. J. F. KNOTT, in "Fundamentals of Fracture Mechanics" (Butterworths, London, 1981) p. 136.
47. G. F. VANDER VOORT, in "Metallography Principles and Practice", (McGraw Hill, New York, 1984) p. 410.
48. JIS G-0555-1977, "Microscopic Testing Method for the Nonmetallic Inclusions in Steels", JIS Handbook, Ferrous Materials and Metallurgy (Japanese Standards Association, 1991).
49. American Society for Testing and Materials, "Standard Methods of Tension Testing of Metallic Materials", E8-87 (ASTM, Philadelphia, PA, 1987).
50. American Society for Testing and Materials, "Standard Methods for Notched Bar Impact Testing of Metallic Materials", E23-86 (ASTM Philadelphia, PA, 1986).

51. D. E. DIESBURG, in "Toughness Characterisation and Specification for HSLA and Structural Steels", edited by P. L. Margonon (American Institute of Mineral Engineers, New York, 1979) p. 19.
52. N. LAZARIDIS and P. L. MARGONON Jr, in "Proceedings of Toughness Characterization and Specifications for HSLA and Structural Steels", Atlanta, GA, March 6–10, 1977, edited by P. L. Margonon Jr (TMS-AIME, Atlanta, Georgia 1979) p. 112.
53. J. C. RADON and C. E. TURNER, *J. Iron Steel Inst.* **204** (1966) 842.
54. R. H. SAILORS and H. T. CORTEN, in "Fracture Toughness", Proceedings of the 1971 National Symposium on Fracture Mechanics, Part II, ASTM STP 514 (American Society for Testing and Materials, Philadelphia, PA, 1972) p. 164.
55. R. J. KLASSEN, M. N. BASSIM and M. R. BAYOUMI, *Mater. Sci. Eng.* **80** (1986) 25.
56. G. T. HAHN and A. R. ROSENFIELD, *Metall. Trans.* **6A** (1975) 653.
57. W. M. GARRISON Jr and N. R. MODY, *ibid.* **18A** (1987) 1257.

Received 30 July 1992
and accepted 26 August 1993